



Comparative analysis of magnetocaloric effect in $\text{La}_{0.67-x}\text{Eu}_x\text{Ba}_{0.33}\text{Mn}_{0.85}\text{Fe}_{0.15}\text{O}_3$ ($x = 0$ and 0.1) polycrystalline manganites: experimental vs. theoretical determination

Aïda Ben Jazia Kharrat¹ · Nassira Chniba-Boudjada^{1,2} · Wahiba Boujelben¹

Received: 28 September 2023 / Accepted: 9 July 2024

© The Author(s), under exclusive licence to Springer Science+Business Media, LLC, part of Springer Nature 2024

Abstract

This research study explores the magnetic and magnetocaloric properties of $\text{La}_{0.67-x}\text{Eu}_x\text{Ba}_{0.33}\text{Mn}_{0.85}\text{Fe}_{0.15}\text{O}_3$ ($x = 0$ and 0.1) magnetic compounds elaborated using the Sol–Gel method, based on a phenomenological approach proposed by Mahmoud Aly Hamad. The studied compounds exhibit a second-order ferromagnetic (FM) to paramagnetic (PM) transition with increasing temperature. A correlation between the experimental measurements and the theoretical analysis is established. Indeed, the value of the magnetocaloric effect was determined from the theoretical model based on magnetization as a function of temperature at several magnetic fields. Under an applied magnetic field of 5T, the absolute values of the maximum magnetic entropy change are evaluated at 0.92 and $0.60 \text{ J kg}^{-1} \text{ K}^{-1}$ for $x = 0$ and 0.1 respectively. This reduction may be attributed to a Curie temperature distribution implying also a decrease in the relative cooling power (RCP). The RCP and the specific heat capacity values are also estimated thanks to this model. The results predicted by this model allow us to propose these compounds as promising candidates for magnetic refrigeration.

Keywords Magnetization · Phenomenological model · Magnetic transition · Specific heat · Magnetocaloric effect

1 Introduction

Mixed-valence manganite compounds possessing the general formula $\text{M}_{1-x}\text{A}_x\text{MnO}_3$ (where M is a rare earth and A denotes an alkaline-earth) were studied for several decades. But, in recent years, they have aroused more interest, as they exhibit exceptionally novel properties such as colossal magnetoresistance (CMR) [1–3] and giant magnetocaloric (MC) effect [4, 5] giving possibility to propose new technological applications. Therefore, many works are conducted on the magnetic and magneto-transport properties of these materials. In addition, the effects of divalent alkaline earth elements have been widely discussed [6–8]. These earlier works have shown that the Curie temperature T_c and the magnetoresistance (MR) effects are optimized for a Mn^{4+} content of about 33%.

Nowadays, magnetic refrigeration has proven to be a promising technology that can replace conventional refrigeration based on gas compression. This new technology, based on magnetic materials, essentially perovskite manganites, notably offers high efficiency, low volume and above all ecological cleanliness [9, 10]. In addition, it can ensure the reduction of greenhouse gases since this new technology does not use toxic gases [11]. Among these manganite materials with high magnetocaloric effect, the $\text{La}_{0.6}\text{Ca}_{0.4-x}\text{Sr}_x\text{MnO}_3$ compounds ($x = 0, 0.05$ and 0.4) [12], the $\text{Pr}_{0.8-x}\text{Bi}_x\text{Sr}_{0.2}\text{MnO}_3$ ($x = 0, 0.05$ and 0.1) [13], $\text{La}_{1-x}\text{K}_x\text{MnO}_3$ ($x = 0.11, 0.13, 0.15$) [14] and $(\text{La}_{1-x}\text{Pr}_x)_{0.67}\text{Pb}_{0.33}\text{MnO}_3$ ($0.0 \leq x \leq 0.3$) [15] compounds.

The LaMnO_3 compound has wide applications in magnetic and technological devices due particularly to its colossal magnetoresistance effect (CMR) as well as its tunable structural and magnetic properties. [16–20].

Boujelben et al. [21] and Ammar et al. [22] studied the substitution effect of manganese by iron in $\text{Pr}_{0.67}\text{Sr}_{0.33}\text{Mn}_{1-x}\text{Fe}_x\text{O}_3$ and $\text{Pr}_{0.5}\text{Sr}_{0.5}\text{Mn}_{1-x}\text{Fe}_x\text{O}_3$ respectively. They demonstrated that this substitution reduces the $\text{Mn}^{4+}/\text{Mn}^{3+}$ ratio and causes a decrease in the Curie temperature in the substituted compounds. Electrical

✉ Aïda Ben Jazia Kharrat
benjaziaaida@gmail.com

¹ Laboratoire de Physique des Matériaux, Faculté des Sciences de Sfax, Université de Sfax, B. P 1171, 3000 Sfax, Tunisia

² Institut Néel, B.P. 166, 38042 Grenoble Cedex 9, France

characterizations show that the substitution of manganese by iron in the $\text{Pr}_{0.67}\text{Sr}_{0.33}\text{Mn}_{1-x}\text{Fe}_x\text{O}_3$ compounds [21] kept the semiconductor–metal transition with a significant reduction in the electrical transition temperature.

Rahmouni et al. have explored the effect of the substitution of manganese by iron (Fe^{3+}) on the electrical properties of the $\text{La}_{0.67}\text{Ba}_{0.33}\text{Mn}_{1-x}\text{Fe}_x\text{O}_3$ ($0 \leq x \leq 0.2$) compounds [23]. This work showed that electrical conductivity decreases with increasing iron concentration. Indeed, the conductivity in manganites is ensured by the double exchange mechanism but for samples whose manganese is doped with iron, the jump of Mn^{3+} electrons to Fe^{3+} is prohibited since the iron eg band is completely filled. The lowering of the conductance is explained by the reduction in concentration of the electrons participating in the jump. In addition, the metal–semiconductor transition is completely suppressed from $x = 0.15$.

For this reason, the $\text{La}_{0.67}\text{Ba}_{0.33}\text{MnO}_3$ compound was investigated in order to study the effect of substituting lanthanum with europium on the structural, electrical and dielectric properties for $x = 0$ and 0.1 . Then, the $\text{La}_{0.67}\text{Ba}_{0.33}\text{MnO}_3$ was chosen to improve the dielectric properties by doping with Eu in A-site and with Fe in B-site. In addition, we focused on the magnetic properties of these compounds to see if these compounds may have multiple properties.

For these compounds, the introduction of Barium and Europium in site A which have different ionic radii ($r_{\text{La}^{3+}} = 1.36 \text{ \AA}$, $r_{\text{Ba}^{2+}} = 1.61 \text{ \AA}$ et $r_{\text{Eu}^{3+}} = 1.12 \text{ \AA}$) causes the variation of the cationic disorder in A-site of the studied compounds leading to a variation in the Curie temperature.

The modification of the cationic disorder in A-site causes variations in the average bond length $\langle \text{Mn-O} \rangle$ and the average angle $\langle \text{Mn-O-Mn} \rangle$ leading to a tilting of the MnO_6 octahedrons.

Concerning manganite materials with ferromagnetic (FM) to paramagnetic (PM) transition, a phenomenological model has been proposed by Mahmoud Aly Hamad [24]. This theoretical model has been tested and has proven its reliability on several manganite compounds. In addition, it is widely used to simulate the temperature evolution of magnetization and to study MC properties, such as magnetic entropy change, relative cooling power (RCP), and heat capacity change [12, 25]. Moreover, this theory has been confirmed for many materials with a magnetic transition such as $\text{Pr}_{0.8-x}\text{Bi}_x\text{Sr}_{0.2}\text{MnO}_3$ ($x = 0, 0.05$ and 0.1) [26], $\text{La}_{0.67}\text{Ca}_{0.33}\text{MnO}_3$ [27], $\text{La}_{0.67}\text{Sr}_{0.33}\text{MnO}_3$ [27] and $\text{La}_{0.7}\text{Ca}_{0.3}\text{MnO}_3$ [28].

On the other hand, the applied magnetic field required to promote MCE in lanthanum manganites is much lower than that required for gadolinium and its alloys [29].

It is important to note that the reliability of the studied model was also confirmed for a magnetic system with multiple magnetic transitions such as charge ordered $\text{Pr}_{0.5}\text{Sr}_{0.5}\text{MnO}_3$ [30] and $\text{Pr}_{0.5-x}\text{Gd}_x\text{Sr}_{0.5}\text{MnO}_3$ ($0 \leq x \leq 0.1$)

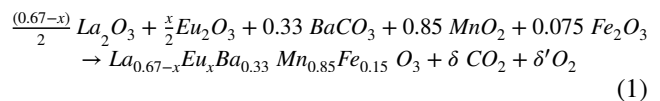
compounds [31]. On the other hand, other works have demonstrated that the proposed phenomenological model is unable to give a rigorous estimate of the magnetocaloric effect in FM materials contrary to what was expected [32]. The unreliability found is attributed not to the phenomenological method but to the erroneous assumption made in the derivation of the entropy change expression, namely that the model parameters are independent of the strength of the applied magnetic field.

The present work is devoted to the verification of a known theoretical model which is the Hamad model to predict the magnetocaloric data of a magnetic material in order to select materials suitable for magnetic refrigeration.

The advantage of Hamad's phenomenological model is that based on theoretical considerations and from a simple measurement of $M(T)$, one can predict whether or not a material exhibits significant magnetocaloric properties. Previous works has also shown that this model is closer to reality than, for example, the Landau model which deviates at low temperature ($T < T_C$) from the experimental curve derived from $M(H, T)$.

2 Experimental details

Polycrystalline samples of nominal composition $\text{La}_{0.67-x}\text{Eu}_x\text{Ba}_{0.33}\text{Mn}_{0.85}\text{Fe}_{0.15}\text{O}_3$ ($x = 0$ and 0.1) were successfully prepared by means of the sol–gel route using high purity (up to 99.9%) dried MnO_2 , La_2O_3 , BaCO_3 , Eu_2O_3 and Fe_2O_3 precursors on the basis of the following chemical reaction:



These samples were elaborated in air, then they can be stoichiometric in oxygen [33].

In a previous work [34], the powder X-ray diffraction (XRD) of these samples, determined at room temperature, was verified, using Cu-K_α radiation ($\lambda = 1.54056 \text{ \AA}$). The obtained results, analyzed by the Rietveld method based on the Fullprof program [35] demonstrated that our samples are single-phase and crystalline in the orthorhombic structure with the $Pbnm$ space group.

The electrical and dielectric properties of these compounds were also studied using the impedance spectroscopy technique in the temperature range of 80 to 400 K and the frequency range of 40 to 10^7 Hz [34]. DC measurements showed that the studied compounds present a semiconductor (SC) behavior in all the temperature range of study. Further, analysis of AC data shows a transition from SC to metallic behavior at the transition temperature $160 < T_{\text{SM}} < 170 \text{ K}$ and $220 < T_{\text{SM}} < 240 \text{ K}$ for $x = 0$ and 0.1 respectively. On the basis of Nyquist plots, an

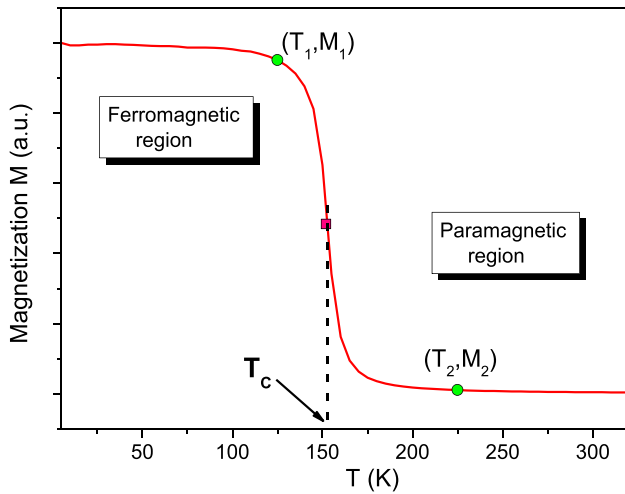


Fig. 1 Evolution of the magnetization curve with temperature T under constant applied magnetic field

equivalent circuit involving the contribution of grains and grain boundaries in the conduction process was proposed. The dielectric measurements revealed also that dielectric relaxation is governed by the DC conduction process. The dielectric results further confirm the high permittivity values which confirm the importance of the studied compounds in electronic applications.

In addition, magnetic measurements were performed using a vibrating sample magnetometer in the temperature range of 5–335 K and under applied magnetic fields up to 7 T.

In this research work and in order to continue our investigation, we used the theoretical phenomenological model of Hamad to simulate experimental results and predict the magnetic, the magnetocaloric properties and the specific heat capacity values of these compounds.

3 Theoretical study

Hamad’s theory [26] was based on the magnetization measurements which evolution with temperature is given by:

$$M(T) = \frac{(M_1 - M_2)}{2} \tanh[A(T_C - T)] + BT + C \quad (2)$$

In this relation:

- (a) M_1 and M_2 designate, the initial and the final magnetizations values at FM and PM transition respectively, as shown in Fig. 1.

- (b) B represents the magnetization sensitivity given by: $B = dM/dT$ in the FM region (before transition).
- (c) The value of C is given by: $C = \frac{(M_1 + M_2)}{2} - B * T_C$.
- (d) $A = 2 \frac{(B - S_C)}{(M_1 - M_2)} - B * T_C$. In this relation, S_C is the magnetization sensitivity at T_C ($S_C = dM/dT$).

According to the studied theory, the magnetic entropy change resulting from the spin ordering under isothermal magnetic field change (varying from 0 to $\mu_0 H_{max}$) is given by the following relation [24]:

$$\Delta S_M(T) = \left[-A \frac{(M_1 - M_2)}{2} \operatorname{sech}^2[A(T_C - T)] + B \right] \mu_0 H_{max} \quad (3)$$

In this relation, $\operatorname{sech}(x) = 1/\cosh(x)$

Among others, at Curie temperature T_C , $\Delta S_M(T)$ reaches its maximum value $\Delta S_{Max}(T)$ given by:

$$\Delta S_{Max}(T) = \left[-A \frac{(M_1 - M_2)}{2} + B \right] \mu_0 H_{max} \quad (4)$$

An important parameter of the isothermal entropy change ΔS is its full width at half maximum δT_{FWHM} determined by: $\Delta S = \Delta S_{Max}(T)/2$ which gives [27, 36]:

$$\delta T_{FWHM} = \frac{2}{A} \cosh^{-1} \left[\sqrt{\frac{2A(M_1 - M_2)}{A(M_1 - M_2) + 2B}} \right] \quad (5)$$

Then, the relative cooling power (RCP) describing the magnetic cooling efficiency of a manganite material can be given by:

$$\begin{aligned} RCP &= -\Delta S_M(T, H_{Max}) \delta T_{FWHM} \\ &= \left(M_1 - M_2 - 2 \frac{B}{A} \right) \mu_0 H_{max} \times \cosh^{-1} \left[\sqrt{\frac{2A(M_1 - M_2)}{A(M_1 - M_2) + 2B}} \right] \end{aligned} \quad (6)$$

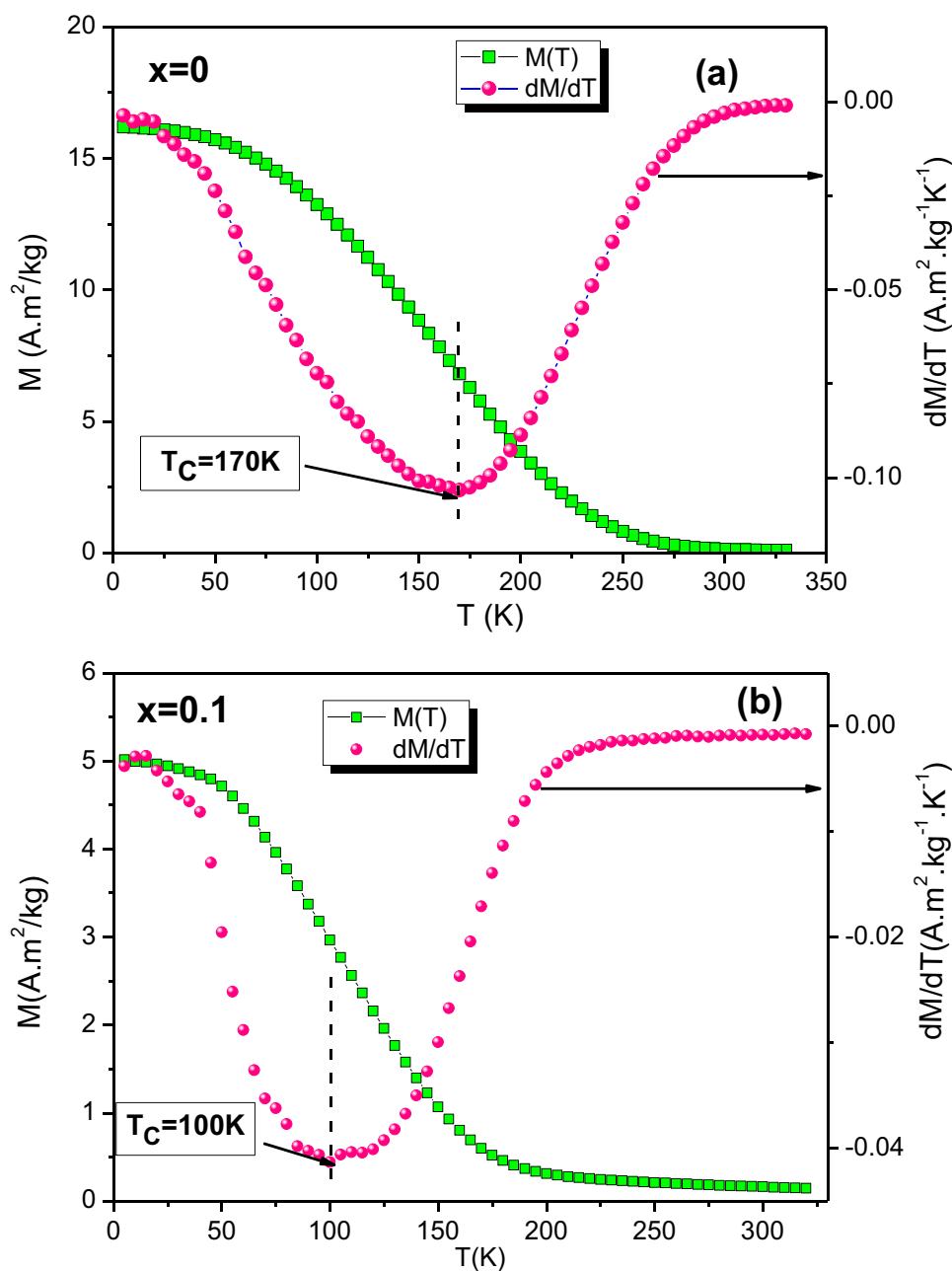
Moreover, the heat capacity which represents also a crucial parameter to assess the importance of a magnetic material, can be determined from the magnetic contribution to $\Delta S_M(T)$ based on the following expression [27]:

$$\Delta C_p(T, \mu_0 H) = C_p(T, \mu_0 H) - C_p(T, 0) = T \frac{\partial [\Delta S_M(T, \mu_0 H)]}{\partial T} \quad (7)$$

This relation can be also written as [13, 37]:

$$\begin{aligned} \Delta C_p(T, \mu_0 H) &= -TA^2 (M_1 - M_2) \times \tanh \\ & \left[A(T_C - T) \right] \mu_0 H_{Max} \operatorname{sech}^2[A(T_C - T)] = T \frac{\partial [\Delta S_M(T, \mu_0 H)]}{\partial T} \end{aligned} \quad (8)$$

Fig. 2 Temperature evolution of the magnetization $M(T)$ determined for the $\text{La}_{0.67-x}\text{Eu}_x\text{Ba}_{0.33}\text{Mn}_{0.85}\text{Fe}_{0.15}\text{O}_3$ ($x=0$ and 0.1) compounds under an applied magnetic field of 0.05 T: **(a)** $x=0$ and **(b)** $x=0.1$. In each figure we have shown the evolution of dM/dT with temperature to determine the Curie temperature T_C



4 Results and discussions

Figure 2(a) and (b) illustrates the evolution of magnetization with temperature under an applied magnetic field of 0.05 T for the $\text{La}_{0.67-x}\text{Eu}_x\text{Ba}_{0.33}\text{Mn}_{0.85}\text{Fe}_{0.15}\text{O}_3$ ($x=0$ and 0.1) studied compounds.

As can be clearly seen, these materials exhibit a FM to PM transition when the temperature increases. On the basis of dM/dT plots, the Curie temperature was estimated for each compound which is 170 K and 100 K for $x=0$ and 0.1 respectively. These determined values will be used to fit the magnetization data as a function of temperature.

Figure 3(a) and (b) demonstrates the evolution of the isothermal magnetization as a function of the applied magnetic field $M(\mu_0 H)$ measured under an applied magnetic fields up to 7 T for our samples. Based on these curves, the temperature dependence of the magnetization $M(T)$ for different applied magnetic fields up to 7 T was plotted in Fig. 4. Using the values extracted from $M(T)$ at $\mu_0 H = 0.05$ T, the magnetization data $M(T)$ for applied magnetic fields varying from 1 to 7 T were simulated on the basis of relation (2). As seen in Fig. 4, a good agreement is obtained between experimental and obtained simulated data. This result confirms the reliability of the phenomenological model proposed by Hamad. The fitted model parameters are gathered in Table 1. This

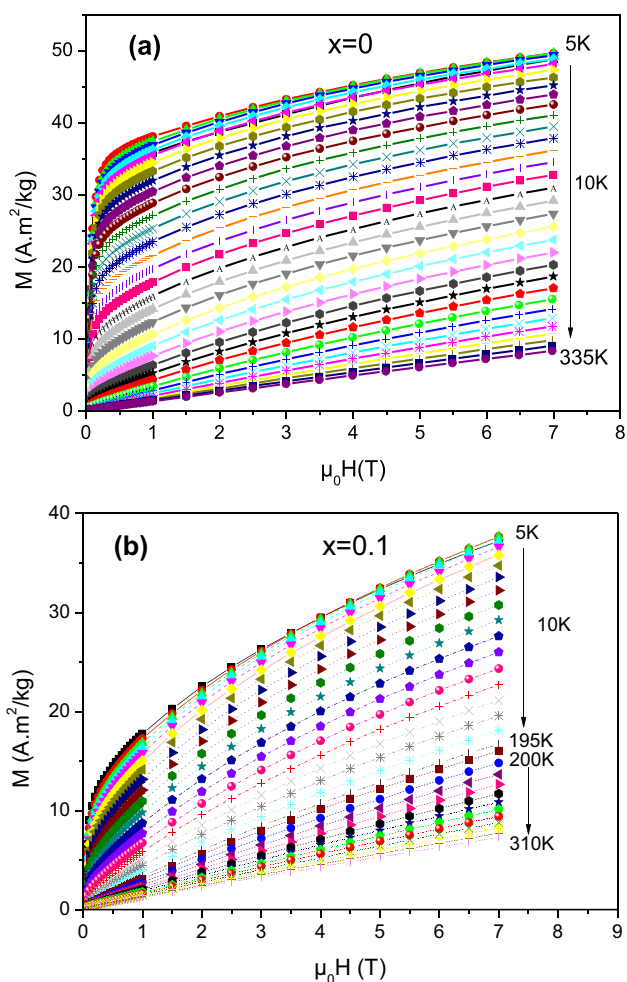


Fig. 3 Isothermal magnetization curves for $\text{La}_{0.67-x}\text{Eu}_x\text{Ba}_{0.33}\text{Mn}_{0.85}\text{Fe}_{0.15}\text{O}_3$ ($x=0$ and 0.1) compounds

agreement was verified also in our previous work with the $\text{Pr}_{0.8-x}\text{Bi}_x\text{Sr}_{0.2}\text{MnO}_3$ ($x=0, 0.05$ and 0.1) compounds [26].

Using the results presented in Table 1, the evolution of the magnetic entropy change ($-\Delta S_M$) with temperature at different applied magnetic fields was calculated using Eq. (3). Obviously, this parameter was determined under the same applied magnetic fields in order to compare the predicted values with those calculated from magnetic measurements.

Results, illustrated in Fig. 5, demonstrate a good agreement between the experimental data and those determined theoretically with the proposed model. Besides, the obtained negative values of the magnetic entropy change confirm the FM behaviour of the samples under investigation [13].

Note especially that the main advantage obtained with this phenomenological model is the prediction of the magnetocaloric properties of any studied compound (possessing magnetic properties) under any applied magnetic field without carrying out the experimental measurements. The obtained results demonstrate that our samples show a

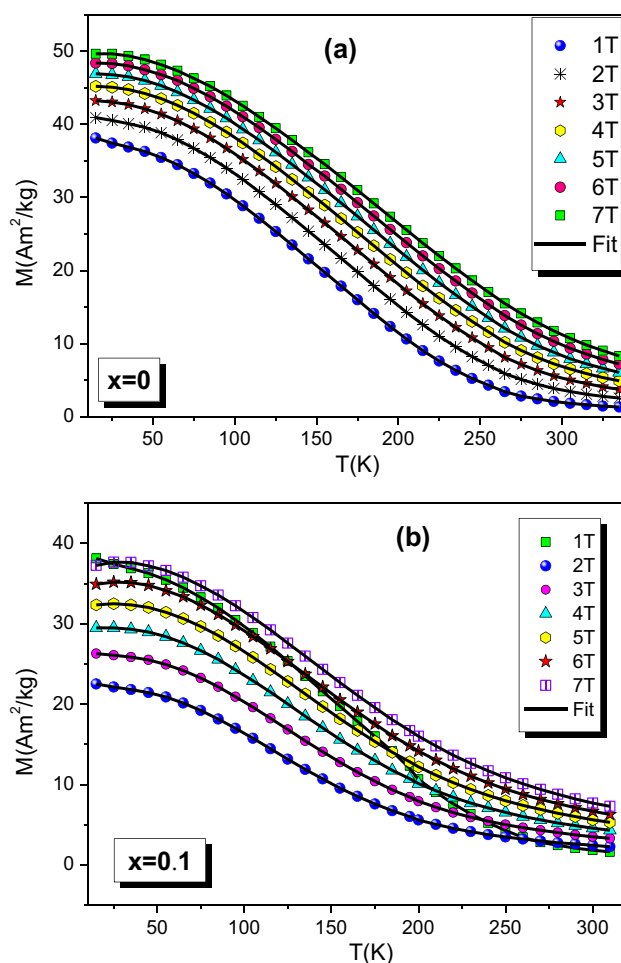


Fig. 4 Temperature dependence of the magnetization at different applied magnetic fields for $\text{La}_{0.67-x}\text{Eu}_x\text{Ba}_{0.33}\text{Mn}_{0.85}\text{Fe}_{0.15}\text{O}_3$ ($x=0$ and 0.1) compounds. Symbols represent the experimental data and solid lines represent the simulated results

large variation in the magnetic entropy change which can be explained by the double exchange mechanism between the Mn^{3+} and Mn^{4+} ions via the oxygen ions proposed by Zener [38]. As known, this model favors FM interactions due for example to the jump of electrons. Indeed, Zener's double exchange mechanism consists in the delocalization of e_g electron, which takes place via the $2p$ orbitals of oxygen ion. The e_g electron hopping promotes the FM interactions and favors metallic tendencies.

It can be noticed that, the evolution of the magnetic entropy change $\Delta S_M(T, \mu_0 H)$ in perovskite magnetic materials, is mainly due to the coupling between the applied magnetic field and the magnetic sublattice. Particularly, this coupling affects the magnetic part of the total entropy due to the evolution of the corresponding magnetic field [39, 40]. Moreover, and as can be seen, $\Delta S_M(T, \mu_0 H)$ is maximal near the Curie temperature T_C corresponding to

Table 1 Parameters fit from Eq. (2) for the $\text{La}_{0.67-x}\text{Eu}_x\text{Ba}_{0.33}\text{Mn}_{0.85}\text{Fe}_{0.15}\text{O}_3$ ($x=0$ and 0.1) compounds at different applied magnetic fields

$\mu_0 H$ (T)	M_I (Am ² /kg)	M_F (Am ² /kg)	T_C (K)	b (Am ² kg ⁻¹ K ⁻¹)	S_C (Am ² kg ⁻¹ K ⁻¹)	R^2
$x=0$						
1	27.01	8.37	160.23	-0.18359	-0.1872	1
2	28.12	14.37	162.57	-0.1824	-0.1808	1
3	28.36	15.97	165.5	-0.17895	-0.1786	1
4	30.77	16.71	167.5	-0.17814	-0.1762	1
5	32.66	17.86	168.75	-0.17023	-0.1703	1
6	33.35	18.22	172.43	-0.16993	-0.1676	1
7	35.66	20.15	173.35	-0.16976	-0.1615	1
$x=0.1$						
1	25.34	12.35	145.24	-0.1667	-0.1864	1
2	22.28	9.30	115.42	-0.1150	-0.1488	1
3	20.14	7.59	124.22	-0.1106	-0.1405	1
4	19.54	7.22	124.94	-0.1025	-0.1374	1
5	18.66	6.98	134.69	-0.08915	-0.13180	1
6	17.12	6.31	135.73	-0.08124	-0.12964	1
7	15.96	5.98	145.24	-0.0796	-0.12045	1

the studied materials where the $M(T)$ curves show a rapid evolution with temperature [41].

Using the magnetocaloric results shown in Fig. 5 and according to Franco and Conde [42], a universal phenomenological curve can be represented based on the following relations:

$$\theta = \begin{cases} -\frac{(T-T_C)}{(T_1-T_C)}, & T \leq T_C \\ \frac{(T-T_C)}{(T_2-T_C)}, & T > T_C \end{cases} \quad (9)$$

In these relations, θ designate the rescaled temperature and T_1 and T_2 are the temperatures of the two reference points obtained for $\Delta S_M = (-\Delta S_M^{Max})/2$. In fact, at fixed applied magnetic field $\mu_0 H$, $\Delta S_M(T)$ is normalized using its peak entropy change $(-\Delta S_M^{Max})$ and the temperature is rescaled below and above the Curie temperature.

Using relation (9), the variation of the normalized entropy change as a function of θ for different applied magnetic fields was reported in Fig. 6.

As clearly illustrated and for each sample, all experimental values collapse into one universal curve which confirms the reversible behavior of the second-order magnetic phase transition for the studied compounds.

On other hand and around T_C , the evolution of the maximum entropy change with the magnetic field can be described with the following expression [43]:

$$-\Delta S_{Max}(T) = \alpha (\mu_0 H)^n \quad (10)$$

In this relation, n depends on the magnetic state of the studied compounds and α is a constant.

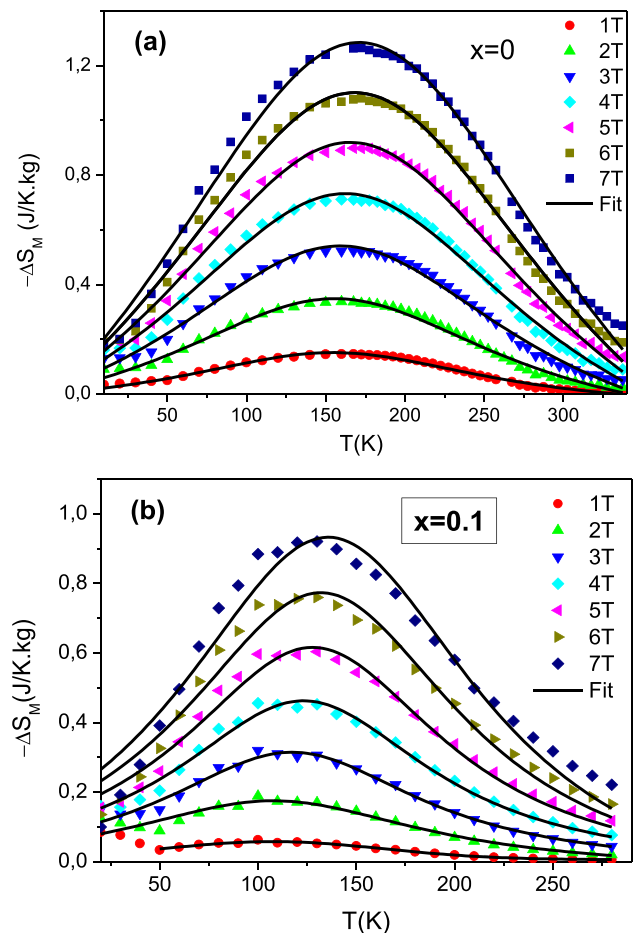


Fig. 5 Temperature dependence of the magnetic entropy change $|\Delta S_M(T)|$ under different applied magnetic fields for $\text{La}_{0.67-x}\text{Eu}_x\text{Ba}_{0.33}\text{Mn}_{0.85}\text{Fe}_{0.15}\text{O}_3$ ($x=0$ and 0.1) compounds **a** $x=0$, and **b** $x=0.1$. Symbols represent the experimental data and solid lines show the predicted values of $|\Delta S_M(T)|$ using Table 1

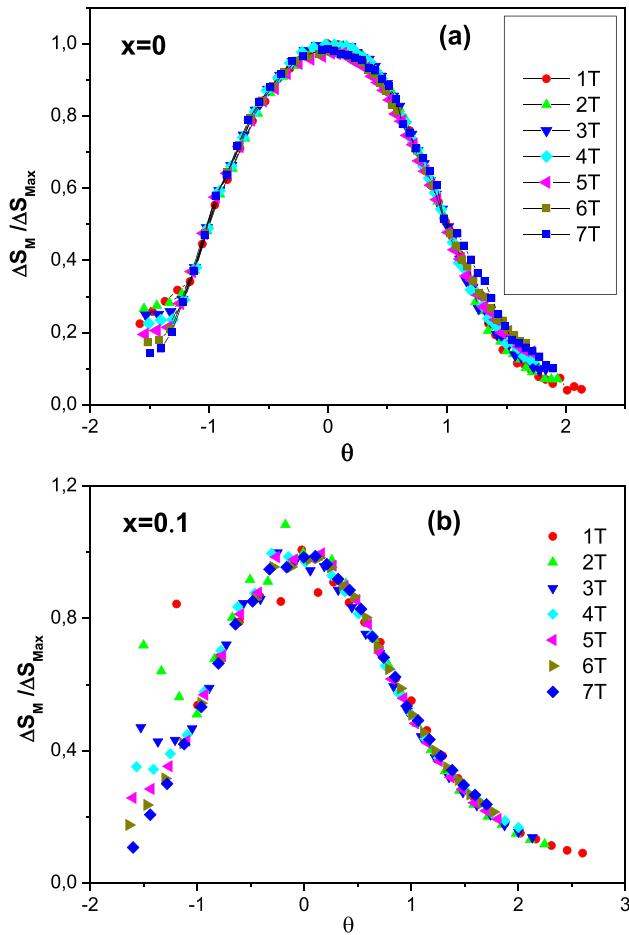


Fig. 6 Normalized entropy change vs. rescaled temperature θ for $\text{La}_{0.67-x}\text{Eu}_x\text{Ba}_{0.33}\text{Mn}_{0.85}\text{Fe}_{0.15}\text{O}_3$ ($x=0$ and 0.1) compounds at different applied magnetic fields

Figure 7 illustrates the variation of the maximum entropy change $|\Delta S_{\text{Max}}|$ and the related fit with relation (10) for $\text{La}_{0.67-x}\text{Eu}_x\text{Ba}_{0.33}\text{Mn}_{0.85}\text{Fe}_{0.15}\text{O}_3$ ($x=0$ and 0.1) compounds at different applied magnetic fields. This fit gives $n=1.0999$ and 1.3089 for $x=0$ and 0.1 respectively.

On the basis of the theoretical ($-\Delta S_M$) values, we have illustrated in Fig. 8, the evolution versus applied magnetic field of δT_{FWHM} and RCP which is considered as the most important parameter to evaluate the MCE relative to our compounds.

As we can notice, the doping with europium reduces the maximum entropy change as well as the δT_{FWHM} which is not beneficial for magnetic refrigeration.

In fact, the reduction in δT_{FWHM} can be explained by the increase in grain size estimated at 22 and 28 nm for $x=0$ and 0.1 , respectively [30]. As a matter of fact, an increase in the particle size induces a reduction in spins near the surface inducing a FM coupling higher than that of bulk grains. Consequently, a Curie temperature distribution may appear which may be the cause of the decrease in $|\Delta S_M|$, δT_{FWHM} and consequently RCP [30].

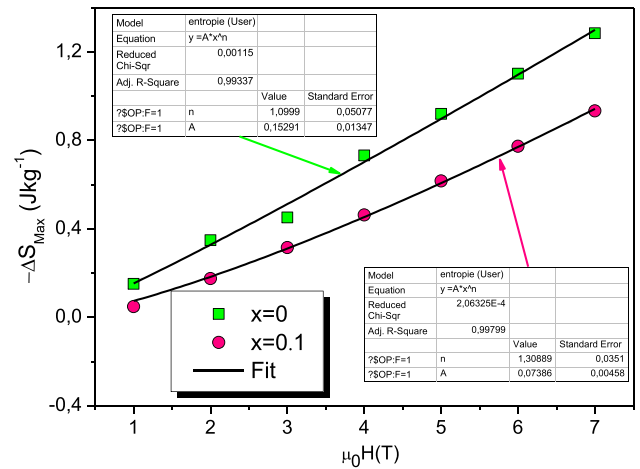


Fig. 7 Evolution of the maximum entropy change $|\Delta S_{\text{Max}}|$ for $\text{La}_{0.67-x}\text{Eu}_x\text{Ba}_{0.33}\text{Mn}_{0.85}\text{Fe}_{0.15}\text{O}_3$ ($x=0$ and 0.1) compounds at different applied magnetic fields

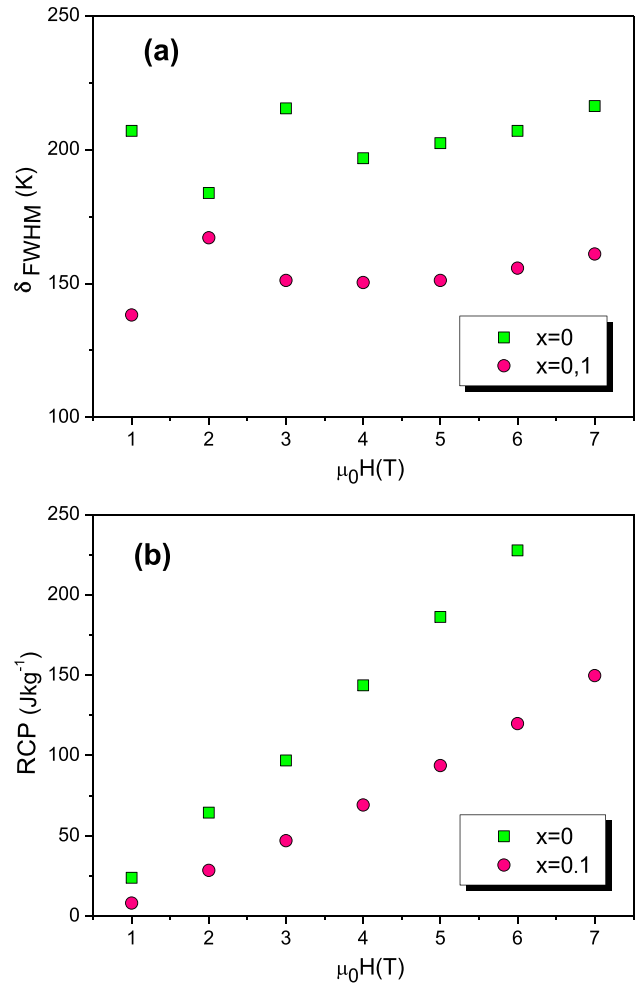


Fig. 8 Evolution of **a** δT_{FWHM} and **b** RCP as a function of applied magnetic field for $\text{La}_{0.67-x}\text{Eu}_x\text{Ba}_{0.33}\text{Mn}_{0.85}\text{Fe}_{0.15}\text{O}_3$ ($x=0$ and 0.1) compounds

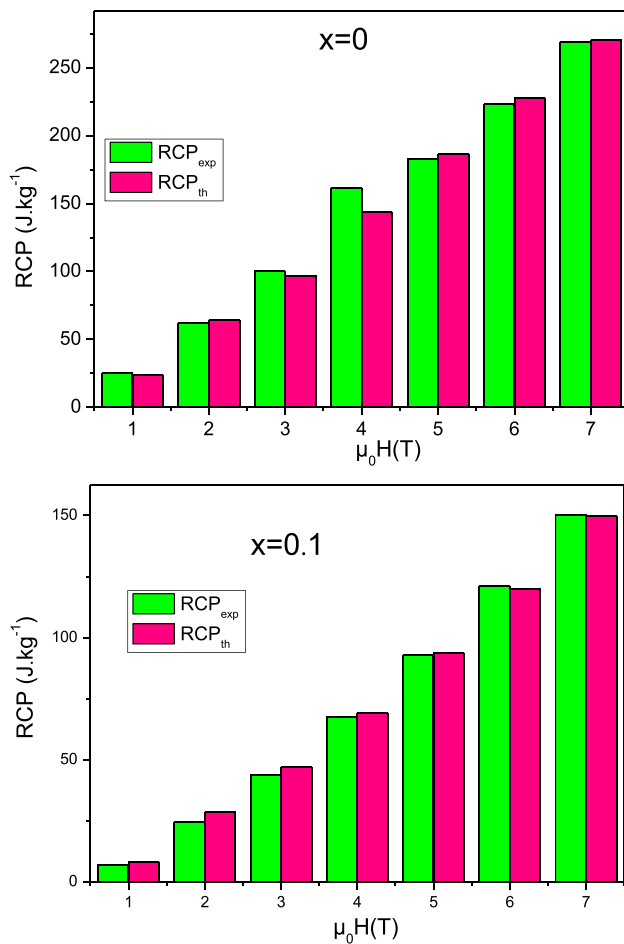


Fig. 9 Comparison between the RCP values obtained from experimental data (RCP_{exp}) and those calculated from the phenomenological model (RCP_{th}) for $La_{0.67-x}Eu_xBa_{0.33}Mn_{0.85}Fe_{0.15}O_3$ ($x=0$ and 0.1) compounds

In Fig. 9, we have compared the theoretical values of RCP calculated with the studied phenomenological model with those obtained from experimental data. A satisfactory agreement is obtained confirming the reliability of the proposed phenomenological model.

This result shows that the RCP values can be predicted directly by the $M(T)$ measurements and subsequently the efficiency of a magnetic material can also be predicted.

Figure 10 shows the evolution of $\ln(RCP)$ vs. $\ln(\mu_0H)$ for $La_{0.67-x}Eu_xBa_{0.33}Mn_{0.85}Fe_{0.15}O_3$ ($x=0$ and 0.1) compounds. The obtained linear fit permits to obtain the critical exponents [23].

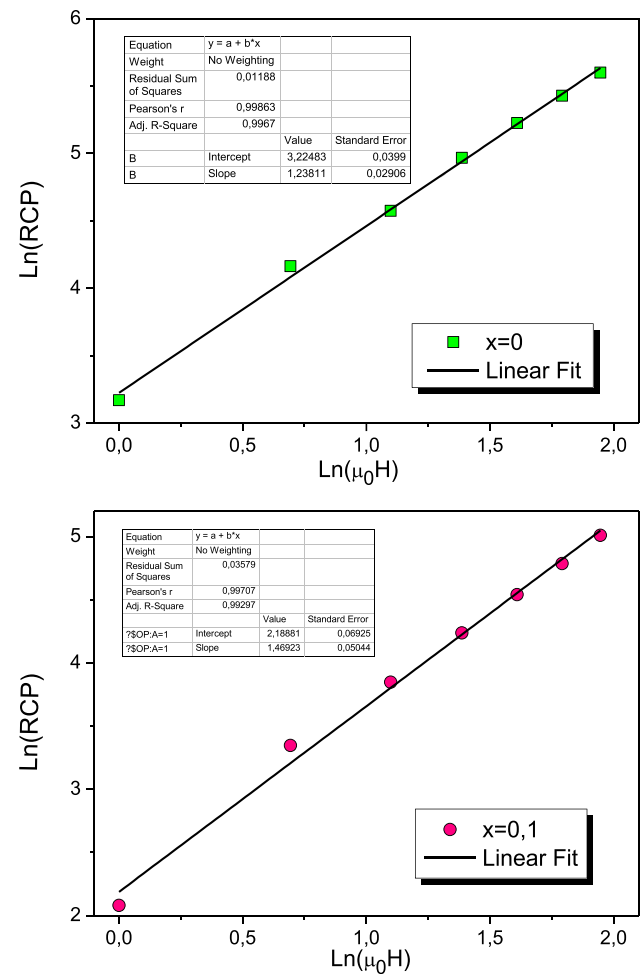


Fig. 10 $\ln(RCP)$ vs. $\ln(\mu_0H)$ for $La_{0.67-x}Eu_xBa_{0.33}Mn_{0.85}Fe_{0.15}O_3$ ($x=0$ and 0.1) compounds

Another important parameter can be predicted from this model instead of doing the experimental measurements is the heat capacity. Indeed, Fig. 11(a) and (b) illustrates the temperature evolution of the predicted heat capacity under different applied magnetic fields relative to the $La_{0.67-x}Eu_xBa_{0.33}Mn_{0.85}Fe_{0.15}O_3$ compounds. As shown, the magnetic field evolution of the specific heat $\Delta C_p(T, \mu_0H)$ deviates from zero only in the vicinity of the transition temperature T_C for the two studied compounds. Besides, $\Delta C_p(T, \mu_0H)$ values are negative below T_C and are positive above.

In Table 2 we have gathered the estimated values of $\Delta C_{p,max}$ and $\Delta C_{p,min}$ at $\mu_0H=5$ T for our studied compounds.

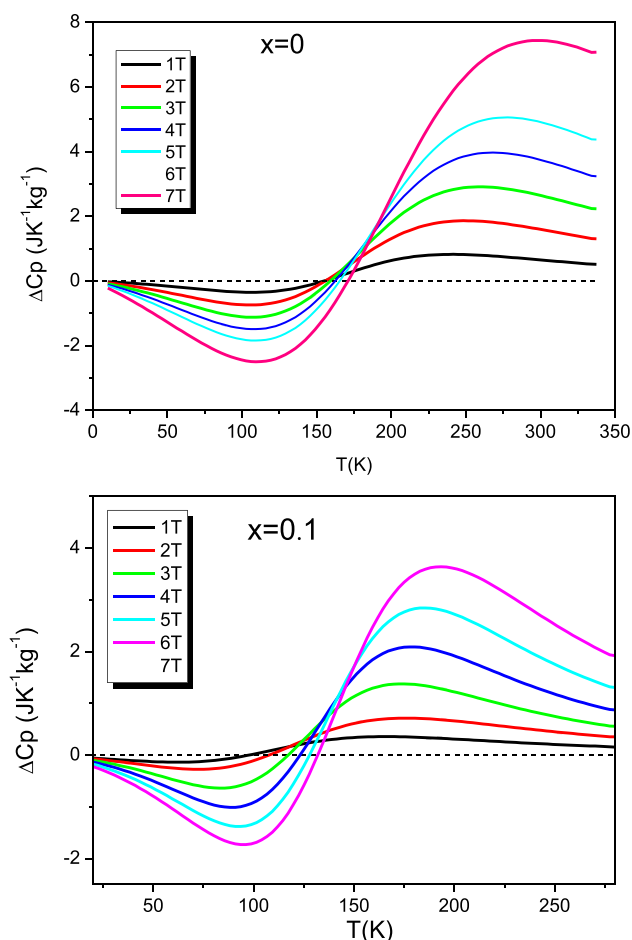


Fig. 11 Temperature evolution of the predicted heat capacity under different applied magnetic fields for the $\text{La}_{0.67-x}\text{Eu}_x\text{Ba}_{0.33}\text{Mn}_{0.85}\text{Fe}_{0.15}\text{O}_3$ compounds **a** $x=0$ and **b** $x=0.1$

Table 2 Specific heat values obtained at $\mu_0H=5\text{T}$ for the $\text{La}_{0.67-x}\text{Eu}_x\text{Ba}_{0.33}\text{Mn}_{0.85}\text{Fe}_{0.15}\text{O}_3$ ($x=0$ and 0.1) compounds

Sample	$\Delta C_{p,\text{max}}$ ($\text{Jkg}^{-1}\text{K}^{-1}$)	$\Delta C_{p,\text{min}}$ ($\text{Jkg}^{-1}\text{K}^{-1}$)	Ref
$x=0$	1.841	-5.0596	This work
$x=0.1$	1.379	-2.846	This work
$\text{Pr}_{0.8}\text{Sr}_{0.2}\text{MnO}_3$	7.541	-6.438	[14]
$\text{Pr}_{0.75}\text{Bi}_{0.05}\text{Sr}_{0.2}\text{MnO}_3$	8.888	-6.600	[14]
$\text{Pr}_{0.7}\text{Bi}_{0.1}\text{Sr}_{0.2}\text{MnO}_3$	9.101	-6.704	[14]

5 Conclusions

In conclusion, we have synthesized polycrystalline manganites with formula $\text{La}_{0.67-x}\text{Eu}_x\text{Ba}_{0.33}\text{Mn}_{0.85}\text{Fe}_{0.15}\text{O}_3$ ($x=0$ and 0.1) using the sol-gel method. Experimental magnetic results show that these compounds exhibit a second order ferromagnetic FM to paramagnetic PM transition with increasing temperature. The magnetic and magnetocaloric properties of these compounds were studied on the basis of the phenomenological model proposed by Mahmoud Aly Hamad.

The present study shows a good agreement between experimental measurements and the magnetic and magnetocaloric results simulated by the studied model.

The full-width at half-maximum, the relative cooling power as well as the specific heat capacity values at several applied magnetic fields is also calculated.

On the basis of the obtained results, the magnetic parameters such as the Curie temperature, around which the application of the magnetic refrigeration is focused, as well as the related parameters of this application can be controlled.

The predicted results are shown to decrease with doping by Europium. Despite that, we can conclude that the prepared compounds may be promising candidates for magnetic refrigeration at low temperatures.

Acknowledgements This work has been supported by the Tunisian Ministry of Higher Education and Scientific Research.

Author contribution Aïda Ben Jazia Kharrat and Nassira Chniba-Boudjada: Conceived and designed the experiments; analyzed and interpreted the data; wrote the paper.

Pr Wahiba Boujelben: Analyzed and interpreted the data; contributed reagents, materials, analysis tools or data; wrote the paper.

Data availability The data that support the findings of this study are not openly available and are available from the corresponding author upon reasonable request.

Declarations

The authors declare that they have no known competing financial interests or personal relationships that could have appeared to influence the work reported in this paper.

Conflict of interest There is no conflict of interest to declare.

References

1. A.P. Ramirez, *J. Phys. Cond. Matt.* **9**, 8171 (1997)
2. J.M.D. Coey, M. Viret, S. von Molnar, *Adv. Phys.* **48**, 167 (1999)
3. A. Ben Jazia Kharrat, E.K. Hlil and W. Boujelben, *Mater. Res. Express* **5**, 126107 (2018)
4. H.O. Wang, Z. Chu, K.P. Su, W.S. Tan, D.X.J. Huo, *J. Alloys Compd.* **689**, 69 (2016)
5. P. Dutta, S. Pramanick, S. Chattopadhyay, D. Das, S.J. Chatterjee, *J. Alloys Compd.* **735**, 2087 (2018)
6. W. Boujelben, A. Cheikh-Rouhou, M. Ellouze, J.C. Joubert, *Phase Transitions* **71**, 127 (2000)
7. W. Boujelben, A. Cheikh-Rouhou, M. Ellouze, J.C. Joubert, *Phys. Stat. Sol. A* **177**, 503 (2000)
8. A. Uruhbarara, Y. Moritomo, T. Arima, A. Asamisu, G. Kido, Y. Tokura, *Phys. Rev. B* **51**, 14103 (1995)
9. M.H. Phan, S.C.J. Yu *Magn. Mater.* **308**, 325 (2007)
10. A. Kitanovski, P.W.J. Ego, *Magn. Mater.* **321**, 777 (2009)
11. H. Zhang, R. Gimaev, B. Kovalev, K. Kamilov, V. Zverev, A. Tishin, Review on the materials and devices for magnetic refrigeration in the temperature range of nitrogen and hydrogen liquefaction. *Phys. Rev. B Condens.* **558**, 65 (2019)
12. H. Gharsallah, M. Beja, E. Dhahri, E.K. Hlil, L. Bessais, Prediction of magnetocaloric effect in $\text{La}_{0.6}\text{Ca}_{0.4-x}\text{Sr}_x\text{MnO}_3$ compounds for $x=0, 0.05$ and 0.4 with phenomenological model. *Ceram. Int.* **42**, 697 (2016)
13. A. Ben Jazia Kharrat, E.K. Hlil, W. Boujelben, Bi doping effect on the critical behavior and magnetocaloric effect of $\text{Pr}_{0.8-x}\text{Bi}_x\text{Sr}_{0.2}\text{MnO}_3$ ($x = 0, 0.05$ and 0.1). *J. Alloys Compd.* **739**, 101 (2018)
14. A.G. Gamzatov, A.M. Aliev, A.R. Kaul, Magnetocaloric effect in $\text{La}_{1-x}\text{K}_x\text{MnO}_3$ ($x=0.11, 0.13, 0.15$) composite structures in magnetic fields up to 80 kOe. *J. Alloys Compd.* **710**, 292 (2017)
15. S.K. Çetin, M. Acet, A. Ekicibil, Effect of Pr-substitution on the structural, magnetic and magnetocaloric properties of $(\text{La}_{1-x}\text{Pr}_x)_{0.67}\text{Pb}_{0.33}\text{MnO}_3$ ($0.0 \leq x \leq 0.3$) manganites. *J. Alloys Compd.* **727**, 1253 (2017)
16. T. Tokura et al., Giant magnetotransport and magnetostructural phenomena in hole-doped manganese oxides. *Mater. Sci. Eng. B* **31**, 187 (1995)
17. M. Viret et al., Magnetic localization in mixed-valence manganites. *Phys. B* **55**, 8067 (1997)
18. D. Varshney, N. Dodiya, M.W. Shaikh, Structural properties and electrical resistivity of Na-substituted lanthanum manganites: $\text{La}_{1-x}\text{Na}_x\text{MnO}_{3+y}$ ($x = 0.1, 0.125$ and 0.15). *J. Alloys Compd.* **509**, 7447 (2011)
19. C. Krishnamoorthy et al., Magnetic and magnetotransport properties of Ce doped nanocrystalline LaMnO_3 . *J. Alloys Compd.* **438**, 1 (2007)
20. J. Töpfer, J.B. Goodenough, Charge transport and magnetic properties in perovskites of the system La–Mn–O. *Solid State Ionics* **101**, 1215 (1997)
21. W. Boujelben, M. Ellouze, A. Cheikh-Rouhou, R. Madar, H. Fuess, *Phys. Stat. Sol. (a)* **201**, 1410 (2004)
22. A. Ammar, S. Zouari, A. Cheikhrouhou, *Phys. Stat. Sol. (c)* **1**, 1645–1648 (2004)
23. H. Rahmouni, B. Cherif, M. Baazaoui, K. Khirouni, *J. Alloys Compd.* **575**, 5 (2013)
24. M.A. Hamad, *Phase Transit.* **87**, 460 (2014)
25. M.A. Hamad, *J. Adv. Ceram.* **4**, 206 (2015)
26. A. Ben Jazia Kharrat, E.K. Hlil, W. Boujelben, *Bull Mater Sci* **42**, 62 (2019)
27. M.A. Hamad, *Phase Transit.* **85**, 106 (2012)
28. M.A. Hamad, *J. Supercond. Nov. Magn.* **27**, 2569 (2014)
29. S.Y. Dan'Kov, A.M. Tishin, V.K. Pecharsky, K.A. Gschneidner, Magnetic phase transitions and the magnetothermal properties of gadolinium. *Phys. Rev. B* **57**(6), 3478 (1998)
30. M. Hsini, S. Hcini, S. Zemni, *J. Magn. Magn. Mater.* **466**, 368 (2018)
31. A. Ben Jazia Kharrat, M. Bourouina, N. Chniba-Boudjada, W. Boujelben, *Solid State Sci.* **87**, 27 (2019)
32. R. Zouari, A. Chehaidar, *Phase Transit.* **90**, 167 (2017)
33. S.V. Trukhanov, I.O. Troyanchuk, N.V. Pushkarev, H.J. Szymczak, *Exp. Theor. Phys.* **95**, 308 (2002)
34. W. Ncib, A. Ben Jazia Kharrat, M.A. Wederni, N. Chniba-Boudjada, K. Khirouni, W. Boujelben, *J. Alloys. Compd.* **768**, 249 (2018)
35. H. Rietveld, *J. Appl. Cryst.* **2**, 65 (1969)
36. M.A. Hamad, *Mater. Lett.* **82**, 181 (2012)
37. W. Zhong, Chen W, Ding W P, Zhang N, Hu A, Du Y W and Yan Q. *J. Eur. Phys. J. B* **3**, 169 (1998)
38. C. Zener, *Phys. Rev.* **82**, 403 (1951)
39. Z.B. Guo, Y.W. Du, J.S. Zhu, H. Huang, W.P. Ding, D. Feng, *Phys. Rev. Lett.* **78**, 1142 (1997)
40. M.S. Reis, V.S. Amaral, J.P. Araújo, P.B. Tavares, A.M. Gomes, I.S. Oliveira, *Phys. Rev. B* **71**, 144413 (2005)
41. K.A. Gschneidner Jr., V.K. Pecharsky, A.O. Tsokol, *Rep. Prog. Phys.* **68**, 1479 (2005)
42. V. Franco, A. Conde, *Int. J. Refrig.* **33**, 465 (2010)
43. Q.Y. Dong, H.W. Zhang, J.R. Sun, B.G. Shen, V.J. Franco, *Appl. Phys.* **103**, 116101 (2008)

Publisher's Note Springer Nature remains neutral with regard to jurisdictional claims in published maps and institutional affiliations.

Springer Nature or its licensor (e.g. a society or other partner) holds exclusive rights to this article under a publishing agreement with the author(s) or other rightsholder(s); author self-archiving of the accepted manuscript version of this article is solely governed by the terms of such publishing agreement and applicable law.